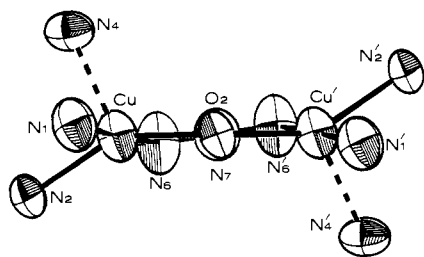


**Figure 1.** ORTEP plot (50%) of the cation  $[\text{Cu}_2(\text{L-Et})(\text{N}_3)]^{2+}$ . A crystallographic  $C_2$  axis passes through atoms N7, O2, and C3. Selected distances (Å): Cu-N1 = 2.06 (1); Cu-N2 = 1.99 (1); Cu-N4 = 2.11 (1); Cu-N6 = 2.04 (1), Cu-O2 = 1.94 (1); Cu...Cu = 3.615 (3); N6-N7 = 1.15 (2). Selected bond angles (deg): O2-Cu-N2 = 143.8 (4); O2-Cu-N6 = 92.3 (5); O2-Cu-N1 = 85.9 (5); O2-Cu-N4 = 114.2 (4); N2-Cu-N6 = 98.8 (5); N2-Cu-N1 = 83.4 (5); N2-Cu-N4 = 98.6 (5); N6-Cu-N1 = 177.8 (5); N6-Cu-N4 = 97.1 (5); N1-Cu-N4 = 82.6 (5); Cu-N6-N7 = 106 (1); Cu-O-Cu = 136.9 (6).



**Figure 2.** ORTEP plot (50%) of the inner coordination sphere viewed down the  $C_2$  axis showing the approximate tetragonal-pyramidal stereochemistry about copper. The longer, axial bond to benzimidazole is identified by the dashed bond. The displacements of the basal donor atoms from the least-squares mean plane of N1, N2, N6, and O2 are as follows: N1, +0.32; N2, -0.29; N6, +0.27; O2, -0.30; Cu, 0.29 Å.

as a mediator of antiferromagnetic coupling,<sup>12,16</sup> we suspect that the alkoxide oxygen atom with its large Cu-O-Cu angle [136.9 (6)°] provides the major superexchange pathway for spin pairing.  $\mu$ -Monohydroxo bridged copper(II) dimers have recently been shown to have similarly large Cu-O-Cu angles (132.2-143.7 Å) and strong antiferromagnetic coupling ( $-J = 161-500 \text{ cm}^{-1}$ ).<sup>21,22,24</sup> The Cu-O-Cu angle in the acetate complex is 130.6°, but, since the alkoxide takes an equatorial site in a ( $d_{z^2}$ )<sup>1</sup> trigonal-bipyramidal ground state, the unpaired electrons do not lie in orbitals collinear with the Cu-O bonds.

The structural data and diamagnetism of the azide complex make it a useful model for both oxy- and methemocyanin derivatives. In azidomethemocyanin it has been anticipated that a 1,3- $\mu$ -azido bridge might easily force the copper atoms >5 Å apart.<sup>5</sup> This is probably the case in ESR-active "dimer" methemocyanin,<sup>5</sup> but the present complex shows that a stable 1,3- $\mu$ -azido bridge could be accommodated with a 3.6-Å Cu...Cu

separation in azidomethemocyanin. Spectroscopically, the azide complex shows considerable similarity to azidomethemocyanin. In acetonitrile solution there is a strong UV maximum at 364 (414 sh) nm ( $\epsilon = 2380 \text{ M}^{-1} \text{ cm}^{-1}$ ), which is not present in the acetate complex. A VIS band is present at 695 nm ( $\epsilon = 195$ ). By comparison to the bands of very similar energy in azidomethemocyanin (*Busycon canaliculatum*) at 360 ( $\epsilon \sim 1500$ ) and 710 nm ( $\epsilon \sim 200$ ),<sup>5</sup> they are assigned to azide LMCT and d-d, respectively. Like other  $\mu$ -1,3-azido copper (II) complexes,<sup>12,16</sup> the present complex has an intense IR band in the region 2020-2040  $\text{cm}^{-1}$  assignable to  $\nu_{\text{asym}} \text{N}_3$  (2020  $\text{cm}^{-1}$ , Nujol mull). This narrow range indicates that  $\nu_{\text{asym}} \text{N}_3$  is not particularly diagnostic of the detailed structure of the 1,3-azido bridge. Since  $\nu_{\text{asym}} \text{N}_3$  in azidomethemocyanin<sup>14</sup> is at 2042  $\text{cm}^{-1}$ , it is not unreasonable to suggest that the present complex and azidomethemocyanin have similar bridge dimensions. The Cu...Cu separation of 3.61 Å in the azide complex is equal to average of the EXAFS determinations (3.55 and 3.67 Å) for two oxyhemocyanins.<sup>6,7</sup> Moreover, the metal-ligand bond lengths (see Figure 1 caption) are very close to those of the most recent EXAFS study of oxyhemocyanin (Cu-N<sub>His</sub> = 2.01; Cu-O<sub>R</sub> = 1.92 Å).<sup>5</sup> A further detail of possible similarity is the  $C_2$  twist of the azide group with respect to the Cu-O-Cu plane (see Figure 2). A similar  $C_2$  twist of the bridging peroxide is a previously favored,<sup>1</sup> but not required,<sup>4</sup> structural feature of oxyhemocyanin. Alkoxide from serine or threonine now becomes a particularly viable candidate for the endogenous bridging ligand R.<sup>23</sup>

Many of the structural features of copper(II) hemocyanin appear to be intrinsic to the coordination chemistry of copper(II) with an appropriate ligand. This augurs well for the model compound approach, and the substitution experiments suggested by the visualized replacement of  $\text{N}_3^-$  by  $\text{O}_2^{2-}$  are under investigation.

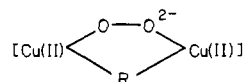
**Acknowledgment.** We are very grateful to Drs. Joseph Waszczak and Frank DiSalvo for low-temperature magnetic measurements and to Professor Edward Solomon for discussion of results prior to publication. This work was supported by the National Science Foundation (CHE 78-09813).

### Competitive Inhibitor Binding to the Binuclear Copper Active Site in Tyrosinase

Marjorie E. Winkler,<sup>1a</sup> Konrad Lerch,<sup>1b\*</sup> and Edward I. Solomon<sup>1a\*</sup>

Department of Chemistry  
Massachusetts Institute of Technology  
Cambridge, Massachusetts 02139  
and Biochemisches Institut der Universität Zurich  
CH-8028 Zurich, Switzerland  
Received June 26, 1981

Recently derivatives of the binuclear copper active site of tyrosinase (monophenol,dihydroxyphenylalanine:oxygen oxidoreductase, EC 1.14.18.1) have been made which parallel those generated for hemocyanin and which exhibit chemical and spectral properties indicative of quite similar active sites. The resting form of tyrosinase is the EPR nondetectable met  $[\text{Cu}(\text{II})\text{Cu}(\text{II})]$  derivative, which can be converted to the oxy derivative by ligand



binding of peroxide. Azide and mimosine (1), inhibitors of tyrosinase, have been shown to displace peroxide from oxytyrosinase

(20) If both azide and acetate structures are considered to be trigonal bipyramidal<sup>19</sup> and if both complexes are assumed to have  $d_{z^2}$  ground states, then the rationale for spin pairing in the azide but not the acetate would require azide to be a markedly superior mediator of antiferromagnetic coupling. While it is presently not possible to dispute this, to our knowledge, there are no examples of diamagnetic trigonal-bipyramidal copper(II) dimers. Thus, we favor the tetragonal rationale presented in the text.

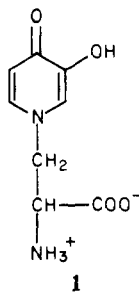
(21) Burk, P. L.; Osborn, J. A.; Youinou, M.-T. *J. Am. Chem. Soc.* **1981**, *103*, 1273-1274.

(22) Haddad, M. S.; Wilson, W. R.; Hodgson, D. J.; Henrickson, D. N. *J. Am. Chem. Soc.* **1981**, *103*, 384-391.

(23) Hydroxide is another possibility.<sup>24</sup> This would make the label "endogenous" inapplicable.

(24) Coughlin, P. K.; Lippard, S. J. *J. Am. Chem. Soc.* **1981**, *103*, 3228-3229.

(1) (a) Massachusetts Institute of Technology. (b) Biochemisches Institut der Universität Zurich, Zurich, Switzerland.



(but not hemocyanin) to yield the met derivative.<sup>2</sup> The EPR detectable  $1/2$ -met [Cu(II)Cu(I)] derivative, formed by the action of  $\text{NaNO}_2$  and ascorbate on met tyrosinase, has been shown to undergo ligand substitution reactions similar to those of  $1/2$ -met hemocyanin.<sup>3-5</sup> The  $1/2$ -met derivatives can be divided into two groups, depending on the nature of the exogenous ligand. In hemocyanin the group I  $1/2$ -met forms ( $\text{NO}_2^-$ ,  $\text{Ac}^-$ ,  $\text{F}^-$ , etc.) have a Cu(II)Cu(I) distance of  $<4 \text{ \AA}$  and coordinate only one ligand per binuclear copper site whereas group II ( $\text{N}_3^-$ ,  $\text{NCS}^-$ , etc.)  $1/2$ -met forms have an estimated Cu(II)Cu(I) distance of  $>5 \text{ \AA}$  and can bind a second ligand weakly.<sup>5</sup> We demonstrate here that mimosine, an inhibitor competitive with organic substrates,<sup>6</sup> competes with azide and peroxide for direct binding to the binuclear copper active site in both the met and  $1/2$ -met derivatives of tyrosinase.

Tyrosinase was purified from cultures of *Neurospora crassa*, and the active site derivatives were formed as described previously.<sup>2,7</sup>

When mimosine is added to oxytyrosinase, a band at 345 nm ( $\epsilon 17000 \text{ cm}^{-1} \text{ M}^{-1}$ ) assigned as a  $\text{O}_2^{2-} \rightarrow \text{Cu}^{2+}$  charge-transfer (CT) transition disappears and a new broad band centered at 420 nm ( $\epsilon 1400 \text{ cm}^{-1} \text{ M}^{-1}$ ) remains. This 420-nm band is observed to grow in ( $\Delta\epsilon 800 \text{ cm}^{-1} \text{ M}^{-1}$ ) when mimosine is added to met-tyrosinase (Figure 1) and is not present in solutions of pure mimosine or enzyme. It must therefore be associated with the mimosine-Cu(II) complex and is evidence for direct binding of mimosine to the binuclear copper site. While resonance Raman studies of met tyrosinase are precluded by protein fluorescence and decay, spectral studies of tetragonal copper(II) model complexes indicate this band to be a phenolate  $\rightarrow$  Cu(II) CT transition.<sup>8</sup>

Excess  $\text{N}_3^-$  displaces the mimosine bound to met tyrosinase, causing the absorption spectrum to change to that of met  $\text{N}_3^-$  (Figure 1). Binding constants for  $\text{N}_3^-$  in the presence of mimosine, determined by use of the  $\text{N}_3^- \rightarrow \text{Cu}^{2+}$  CT transition at 360 nm ( $\Delta\epsilon 2100 \text{ cm}^{-1} \text{ M}^{-1}$ ) indicate that mimosine and azide compete for the same binding site,<sup>9</sup> which is also the binding site of peroxide. No EPR signal is observed at 7 K when mimosine or  $\text{N}_3^-$  are bound to met tyrosinase, and there is no evidence for a ternary complex of  $\text{N}_3^-$ , mimosine, and met tyrosinase.

Addition of mimosine to the  $1/2$ -met  $\text{NO}_2^-$  derivative of tyrosinase yields new bands in the absorption spectrum at 430 and 360 nm. The band at 430 nm is similar to that observed in the met derivative, indicative of mimosine binding to the  $\text{Cu}^{2+}$  in  $1/2$ -met tyrosinase.<sup>10</sup> The EPR spectrum of the  $1/2$ -met mimosine

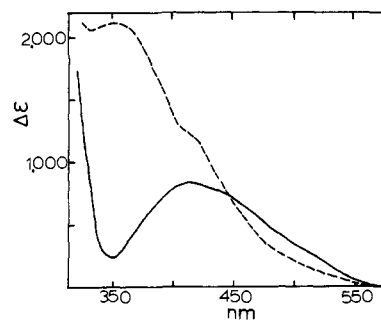


**Figure 1.** Optical absorption difference spectra of the charge-transfer region of (—) met mimosine and (---) met mimosine + 500-fold excess  $\text{N}_3^-$ , *Neurospora* tyrosinase, pH 6.3 phosphate buffer. The reference is met aquo tyrosinase, formed by addition of excess mimosine and then excess  $\text{N}_3^-$  to oxytyrosinase, followed by Sephadex G-25 chromatography.

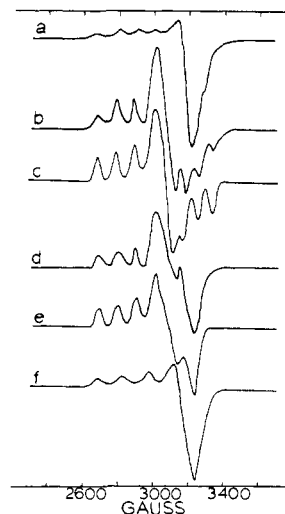


**Figure 2.** EPR spectra of  $1/2$ -met tyrosinase. (a)  $1/2$ -met  $\text{N}_3^-$  after passage through Sephadex G-25; (b) same sample as in (a) + excess mimosine, yielding  $1/2$ -met mimosine; (c) computer simulation of (b), parameters given in text; (d)  $1/2$ -met mimosine +  $\text{N}_3^-$  ternary complex; (e) computer simulation of (d), parameters given in text; (f)  $1/2$ -met mimosine + excess  $\text{N}_3^-$  after 24 h.

derivative (Figure 2) shows a large rhombic distortion and a four line splitting pattern in the perpendicular region. Because there is no evidence of an intervalent transfer transition in the near IR absorption spectrum, the splitting is assigned as hyperfine splitting from Cu(II) rather than superhyperfine splitting from the adjacent Cu(I). Computer simulations give EPR parameters as  $g_z = 2.290$ ,  $g_x = 2.115$ ,  $g_y = 2.023$ ,  $A_z = 111.3 \times 10^{-4} \text{ cm}^{-1}$ ,  $A_x = 15.0 \times 10^{-4} \text{ cm}^{-1}$ , and  $A_y = 72.0 \times 10^{-4} \text{ cm}^{-1}$ .

The EPR spectrum of  $1/2$ -met mimosine in excess mimosine does not change upon passing the derivative through Sephadex G-25, indicating that only one molecule of mimosine binds to the binuclear site, as group II behavior predicts a second ligand would be weakly bound and therefore easily removed.<sup>2</sup> When excess  $\text{N}_3^-$  is added to the  $1/2$ -met mimosine derivative, however, the EPR spectrum changes to one which cannot be assigned as  $1/2$ -met mimosine,  $1/2$ -met  $\text{N}_3^-$ , or a mixture of these spectra, demonstrating that a ternary complex has been formed. The EPR spectrum (Figure 2) shows almost the same rhombic splitting as observed for  $1/2$ -met mimosine except that the perpendicular hyperfine splittings have been reduced ( $g_z = 2.290$ ,  $g_x = 2.130$ ,  $g_y = 2.025$ ,  $A_z = 111.3 \times 10^{-4} \text{ cm}^{-1}$ ,  $A_x = 15.0 \times 10^{-4} \text{ cm}^{-1}$ , and  $A_y = 15.0 \times 10^{-4} \text{ cm}^{-1}$ ). Optically, the addition of  $\text{N}_3^-$  to  $1/2$ -met

(2) Himmelwright, R. S.; Eickman, N. C.; LuBien, C. D.; Lerch, K.; Solomon, E. I. *J. Am. Chem. Soc.* **1980**, *102*, 7339-7344.

(3) Himmelwright, R. S.; Eickman, N. C.; Solomon, E. I. *Biochem. Biophys. Res. Commun.* **1978**, *81*, 237-242.

(4) Himmelwright, R. S.; Eickman, N. C.; Solomon, E. I. *Biochem. Biophys. Res. Commun.* **1978**, *84*, 300-305.

(5) Himmelwright, R. S.; Eickman, N. C.; Solomon, E. I. *J. Am. Chem. Soc.* **1979**, *101*, 1576-1586.

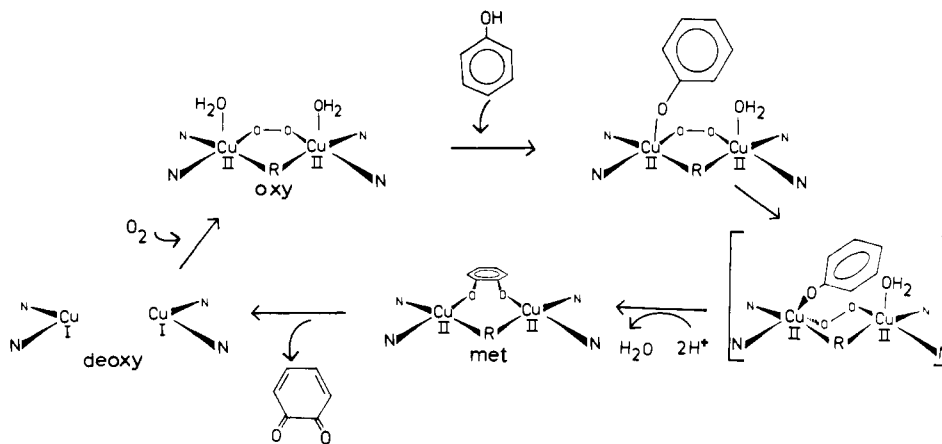
(6) Hashiguchi, H.; Takahashi, H. *Mol. Pharmacol.* **1977**, *13*, 362-367.

(7) Eickman, N. C.; Solomon, E. I.; Larrabee, J. A.; Spiro, T. G.; Lerch, K. *J. Am. Chem. Soc.* **1978**, *100*, 6529-6531.

(8) (a) Solomon, E. I. In "Copper Proteins"; Spiro, T. G., Ed.; Wiley: New York, in press. (b) Amundsen, A. R.; Whelan, J.; Bosnich, B. *J. Am. Chem. Soc.* **1977**, *99*, 6730-6739.

(9)  $K_{\text{N}_3^-} = 3000 \text{ M}^{-1}$  when  $[\text{mimosine}] = 0$ ,  $K_{\text{N}_3^-} = 125 \text{ M}^{-1}$  when  $[\text{mimosine}] = 3 \times [\text{tyrosinase}]$ , and  $K_{\text{N}_3^-} = 20 \text{ M}^{-1}$  when  $[\text{mimosine}] = 20 \times [\text{tyrosinase}]$ .

(10) We do not report  $\Delta\epsilon$  values for the new bands at 430 and 360 nm in  $1/2$ -met mimosine tyrosinase because reliable difference spectra cannot be obtained. (Half-met tyrosinase contains  $\sim 10$ -20% oxytyrosinase, and therefore has an intense peak at 345 nm which is displaced by mimosine. Because of the tight binding of mimosine and other exogenous ligands, a pure  $1/2$ -met aquo sample cannot be obtained as a reference.)

Scheme I. Proposed Mechanism of Hydroxylation and Oxidation of Phenols to Form *o*-Diquinones by *Neurospora* Tyrosinase

mimosine causes a new band to grow in at 350 nm ( $\Delta\epsilon$  2500  $\text{cm}^{-1} \text{M}^{-1}$ ), and "d-d" bands are observed centered around 700 nm.<sup>11</sup> No new bands are observed around 500 nm expected for a bridging  $\text{N}_3^-$ ,<sup>2</sup> and the  $\text{N}_3^-$  is removed by passage through Sephadex G-25. Therefore  $\text{N}_3^-$  is weakly bound to the  $1/2$ -met site as would be predicted for group II behavior of mimosine.

Group II behavior requires that upon ligand binding the Cu(I)Cu(II) distance increases to  $> 5 \text{ \AA}$ .<sup>5</sup> This cannot be done by bridging the coppers through the two aromatic oxygens of mimosine and therefore suggests a geometry where one phenolate oxygen binds to the Cu(II) (required by the phenolate  $\rightarrow$  Cu(II) CT transition at 430 nm) and perhaps the carboxylate binds to the Cu(I). The geometry around the Cu(II) must be quite distorted as evidenced by the rhombic splittings and perpendicular hyperfine structure in the EPR. A Cu(II)Cu(II) distance of  $> 5 \text{ \AA}$  is not consistent with the lack of EPR signal in the met mimosine derivative. In this case the mimosine probably binds to the binuclear copper center through one or both aromatic oxygens.

After 24 h in the presence of 300-fold excess  $\text{N}_3^-$ , the  $1/2$ -met mimosine complex does convert to the  $1/2$ -met  $\text{N}_3^-$  form of tyrosinase as evidenced by EPR (Figure 2). As with the met mimosine derivative,  $\text{N}_3^-$  displaces mimosine, again indicating that  $\text{N}_3^-$ , mimosine, and peroxide all compete for the same binding site at the binuclear copper active site of tyrosinase.

In our earlier studies which probed small molecule binding to the tyrosinase site, a structural mechanism was proposed which predicted that both the small molecule and the organic substrate would first bind associatively to an axial position at the tetragonal cupric site and then rearrange through a trigonal-bipyramidal intermediate to the same equatorial binding site.<sup>2</sup> In this communication we have demonstrated that the competitive inhibitor mimosine does indeed bind equatorially to the binuclear copper center in both the met and the  $1/2$ -met derivatives and competes with the small molecules azide and peroxide for the same binding site. These results lead to the mechanism outlined in Scheme I as the pathway for hydroxylation and oxidation of phenols by tyrosinase. In an associative rearrangement through a trigonal-bipyramidal intermediate, the monophenol labilizes the peroxide from one copper, leaving a reactive polarized peroxide which can hydroxylate the phenol. Oxidation of the resulting diphenol would then occur from the equatorial position, and the *o*-quinone would likely leave dissociatively from the reduced binuclear cuprous site, allowing further turnover. Inhibitors, however, would not be oxidized and would therefore only be displaced from the active site by other exogenous ligands. It has been suggested that mimosine cannot displace  $\text{O}_2^{2-}$  from the binuclear copper center in hemocyanin because of poor accessibility of this site.<sup>2</sup> This suggestion would also be consistent with the above model of

substrate binding to tyrosinase.

**Acknowledgment.** We are grateful to the National Institute of Arthritis, Metabolism and Digestive Diseases (Grant AM20406-05) and the Swiss N.S.F. (Grant 3.420.78) for support of this research. M.E.W. acknowledges the N.I.H. for a post-doctoral fellowship.

### Novel Intramolecular Photorearrangement of Alkane Nitronate Anions

K. Yamada,\* T. Kanekiyo, S. Tanaka, K. Naruchi, and M. Yamamoto

Department of Industrial Chemistry  
Faculty of Engineering, The University of Chiba  
Yayoicho, Chiba 260, Japan  
Received March 31, 1981

We wish to report about the photorearrangement of alkane nitronate anions<sup>1</sup> which provides an interesting synthetic method of introducing hydroxamic acid functions. The nitronate anion **8**, produced from 2-nitro-1,7,7-trimethylbicyclo[2.2.1]heptane (**7**) in an EtOH-EtONa solution, showed a strong UV absorption at 240 nm ( $\epsilon$  12 800)<sup>2</sup> and was transformed to 2-hydroxy-1,8,8-trimethyl-2-azabicyclo[3.2.1]octan-3-one (**10**)<sup>3</sup> by irradiation with a low-pressure mercury lamp. Because it was reported that nitrones undergo photoisomerization to oxaziridines and then decompose to amides, this photoprocess was expected to involve *O*-oxaziridines (**II**)<sup>4</sup> (Scheme I).

A typical photoreaction procedure is as follows: A solution of 2-nitro-1,7,7-trimethylbicyclo[2.2.1]heptane (**7**) ( $[\alpha]_{\text{D}}^{18} + 9.4^\circ$  (EtOH))<sup>5</sup> (1.14 g) in EtOH-EtONa was irradiated for 4.5 h. After irradiation the solution was neutralized with 0.1 M AcOH in EtOH. Solvent removal followed by extraction from the residue with  $\text{CHCl}_3$  gave a white solid (1.09 g) which was chromatographed<sup>6</sup> on silica gel to yield 0.71 g of *N*-hydroxy lactam **10**

(1) The formation of the nitronate anions largely depends on the kinetic acidity. Flanagan, P. W. K.; Amburn, H. W.; Stone, H. W.; Traynham, J. G.; Schechter, H. *J. Am. Chem. Soc.* **1969**, *91*, 2797.

(2) William, F. T., Jr.; Flanagan, P. W. K.; Taylor, W. J.; Schechter, H. *J. Org. Chem.* **1965**, *30*, 2674.

(3) An authentic sample prepared according to the literature was identical in all aspects with **10**. Nakazaki, M.; Naemura, K. *Bull. Chem. Soc. Jpn.* **1964**, *37*, 532.

(4) (a) Spence, G.; Taylor, C.; Buchardt, O. *Chem. Rev.* **1970**, *70*, 231.

(b) Kikuchi, O.; Tanaka, S.; Naruchi, K.; Yamada, K. *J. Fac. Eng. Chiba Univ.* **1981**, *32*, 55.

(5) Forster, M. O. *J. Chem. Soc.* **1900**, 75, 251.

(6) Flash chromatography was employed for the separation of all the photoproducts. Still, W. C.; Kahn, M.; Mitra, A. *J. Org. Chem.* **1978**, *43*, 2923.

(11) From the equations  $g_x = 2.0023 + 2\zeta/(E_{xy} - E_{xz})$  and  $g_y = 2.0023 + 2\zeta/(E_{xy} - E_{yz})$  we estimate a 1500- $\text{cm}^{-1}$  shift of the "d-d" bands to higher energy of  $1/2$ -met mimosine relative to the ternary complex of  $1/2$ -met mimosine and azide.